

## MIT Open Access Articles

### *Electron-beam Directed Materials Assembly*

The MIT Faculty has made this article openly available. **Please share** how this access benefits you. Your story matters.

**Citation:** Kingsborough, Richard P. et al. "Electron-beam directed materials assembly." Alternative Lithographic Technologies II. Ed. Daniel J. C. Herr. ©2010 SPIE

**As Published:** <http://dx.doi.org/10.1117/12.846000>

**Publisher:** SPIE

**Persistent URL:** <http://hdl.handle.net/1721.1/58610>

**Version:** Final published version: final published article, as it appeared in a journal, conference proceedings, or other formally published context

**Terms of Use:** Article is made available in accordance with the publisher's policy and may be subject to US copyright law. Please refer to the publisher's site for terms of use.



# Electron-beam directed materials assembly

Richard P. Kingsborough, Russell B. Goodman, David Astolfi, and Theodore H. Fedynyshyn

Lincoln Laboratory, Massachusetts Institute of Technology  
Lexington, MA 02420

## ABSTRACT

We have developed a processing method that employs direct surface imaging of a surface-modified silicon wafer to define a chemical nanopattern that directs material assembly, eliminating most of the traditional processing steps. Defining areas of high and low surface energy by selective alkylsiloxane removal that match the polymer period length leads to defect-free grating structures of poly(styrene-*block*-methyl methacrylate) (PS-*b*-PMMA). We have performed initial studies to extend this concept to other wavelengths beyond 157 nm. In this present paper, we will show that electron beam lithography can also be used to define chemical nanopatterns to direct the assembly of PS-*b*-PMMA films. Half-pitch patterns resulted in the directed assembly of PS-*b*-PMMA films. Electron beam lithography can also be used to prepare surfaces for pitch division. Instead of the deposition of an HSQ pinning structure as is currently done, we will show that by writing an asymmetric pattern, we can fill in the space with smaller lamellar period block copolymers to shrink the overall pitch and allow for 15-nm features.

**Key words:** Block copolymer, directed self-assembly

## 1. INTRODUCTION

Symmetric diblock copolymers have been studied for their ability to phase separate into lamellar microdomains with dimensions on the order of 10-50 nm.<sup>1-9</sup> It is possible to use these microdomains to extend pattern formation to critical dimensions smaller than with current optical lithography techniques.<sup>2,11-12</sup> Selective removal of one of the blocks<sup>2</sup> results in templates that can be used in further nanofabrication processes. One of the most studied systems for templating block copolymers has been poly(styrene-*block*-methyl methacrylate) (PS-*b*-PMMA).<sup>2-9,12</sup> A number of research groups have been investigating chemical nanopatterning of a silicon surface by the selective functionalization of a grafted random copolymer brush<sup>3-5</sup> or self-assembled monolayer<sup>3,5,13-15</sup> as templates to direct the self-assembly of block copolymers. We recently reported a patterning method that uses a photoactive alkylsiloxane-modified surface in place of the copolymer brush.<sup>16,17</sup> On this modified silicon surface, we can directly form a surface energy image by conventional lithographic exposure, e.g., interference lithography. In this method, the dose delivered to the surface modifying agent varies continuously along the path of the aerial image, with areas of hydrophilic and hydrophobic surfaces that are separated by areas of intermediate surface energy. Thus, we generate a surface with continuously changing surface energy compared to a conventional binary surface energy approach using chemically nanopatterned polymer brushes.

A great deal of work has been done in the area of patterning surface-modified silicon wafers.<sup>18</sup> Previous research has shown that alkyl- and arylsiloxane self-assembled monolayers can be patterned upon exposure to 157-nm irradiation,<sup>16-17,19-21</sup> as well as other exposure techniques including 193-nm irradiation,<sup>22-28</sup> and e-beam patterning.<sup>29-33</sup> In many cases, photopatterning occurs through the cleavage of the Si-C bond. The degree of Si-C bond cleavage was proportional to the exposure dose applied. This was extended to 157-nm interference lithography to directly pattern an *n*-butylsiloxane-modified silicon surface to generate templates for the directed assembly of polystyrene-*block*-poly(methyl methacrylate) (PS-*b*-PMMA) into grating patterns.<sup>16,17</sup> We now extend this methodology to electron beam lithography and show that patterning an alkylsiloxane-modified surface, in concert with an UV/ozone development step, results in the directed self-assembly of PS-*b*-PMMA films into periodic ordered structures.

## 2. EXPERIMENTAL

Silicon wafers were cleaned by immersion into CD26 developer for 10 minutes at room temperature to hydroxylate the silicon surface, rinsed with deionized water and blown dry under a stream of nitrogen. CD26 is a commercial, surfactant-free 2.38% tetramethylammonium hydroxide (TMAH) based aqueous resist developer from Rohm and Haas. A 1% (v/v) solution of *n*-butyltrichlorosilane (Gelest) in toluene was prepared and allowed to mature for 10 minutes. The cleaned silicon wafer was immersed in the *n*-butyltrichlorosilane solution for 20 minutes, rinsed with toluene and blown dry under a stream of nitrogen. Bulk exposure was performed at 157 nm with a laboratory-class projection system employing an F<sub>2</sub> laser. Once exposed, the wafer was rinsed with deionized water and blown dry with a stream of nitrogen. Electron-beam patterning of the modified silicon surface was performed on a JBX6000FS electron beam exposure system at 50 kV accelerating voltage. After exposure, the electron-beam damaged areas were cleaned out with exposure to UV-ozone using a Novascan PSD-UV3 Digital UV Ozone System. Contact angle measurements were performed using deionized water and decalin. In a typical measurement, a 1 μL drop of water was placed on the surface being measured using a microsyringe. On a microscope stage equipped with a Boeckler Instruments Microcode II measurement device, the *x*- and *y*-diameters were measured and averaged according to  $d = (x^2 + y^2)^{1/2}$ . This diameter value was converted to a contact angle according to Bikerman's equation<sup>34</sup> (Eq. 1) where *d* is the diameter of the drop and *V* is the volume of the drop. After the water and decalin contact angles were determined, the polar and dispersive surface energies for a given surface were calculated by the method of Fowkes.<sup>35-36</sup>

$$\frac{d^3}{V} = \frac{24 \sin^3 \theta}{\pi(2 - 3 \cos \theta + \cos^3 \theta)} \quad (1)$$

Symmetric poly(styrene-*block*-methyl methacrylate) (PS-*b*-PMMA) block copolymers were purchased from Polymer Source Inc. and had a molecular weight of (50.6-*b*-47.6) kg/mol with a polydispersity index of 1.13 and bulk lamellar repeat periods of  $L_0 = 45$  nm. Thin films of PS-*b*-PMMA were spin coated onto the desired substrate to give films that were approximately 20-45 nm thick. The thicknesses of the films were determined using a Gaertner Scientific Corporation L115BLC Dual Wavelength Ellipsometer using a He-Ne laser ( $\lambda=632.8$  nm) at an incident angle of 70° relative to the surface normal of the substrates. The polymer films were then annealed at 260 °C for 2 hrs on a hotplate in a nitrogen-filled glove box. After annealing, the films were imaged using a LEO-1525 field-emission scanning electron microscope (SEM) at an accelerating voltage of 1 kV.

## 3. RESULTS AND DISCUSSION

Electron beam lithography has been previously used to remove selected areas of a self-assembled monolayer. These opened areas have been used as etch masks<sup>31,32</sup> as well as for patterning bioactive templates with a non-active area.<sup>29,30</sup> Exposure of a self-assembled monolayer to high-energy electrons results in the cleavage of C-H bonds along the alkyl chain as well as the formation of a carbonaceous residue at high exposure doses.<sup>33</sup> In order to make use of the exposed areas as etch masks, an all-dry UV/ozone development step was used to remove this residual carbon material.<sup>31,32</sup> Because the polar surface energy plays an important role in PS-*b*-PMMA lamellar orientation,<sup>16</sup> we have investigated the effect of UV/ozone exposure on an *n*-butylsiloxane-modified surface. A plot of polar surface energy as a function of UV/ozone exposure time for an *n*-butylsiloxane-modified silicon wafer is shown in Figure 1a. At low exposure times (< 30 sec), there is little change in the polar surface energy from the initial 0.4 dyne/cm. At longer times, the polar surface energy increases from 0.8 dyne/cm at 30 sec to 8.5 dyne/cm after 180 sec. Much longer exposure times (>15 min) result in the polar surface energy leveling out near 20 dyne/cm, indicative of an oxygen-containing terminal functionalization.<sup>33</sup> Figure 1b shows similar polar surface energy changes as a function of 157-nm exposure.<sup>16</sup> In this case, the exposure to 157-nm light cleaves the Si-C bond, with the Si quickly reacting with water to form SiOH.<sup>16-17,19-21</sup> The amount of alkylsiloxane that is removed is a function of the exposure dose at 157 nm. Unlike exposure to UV/ozone, high exposure doses at 157 nm result in the complete removal of the *n*-butylsiloxane surface modifier and a surface energy approaches that of bare SiO<sub>2</sub> (ca. 42 dyne/cm).

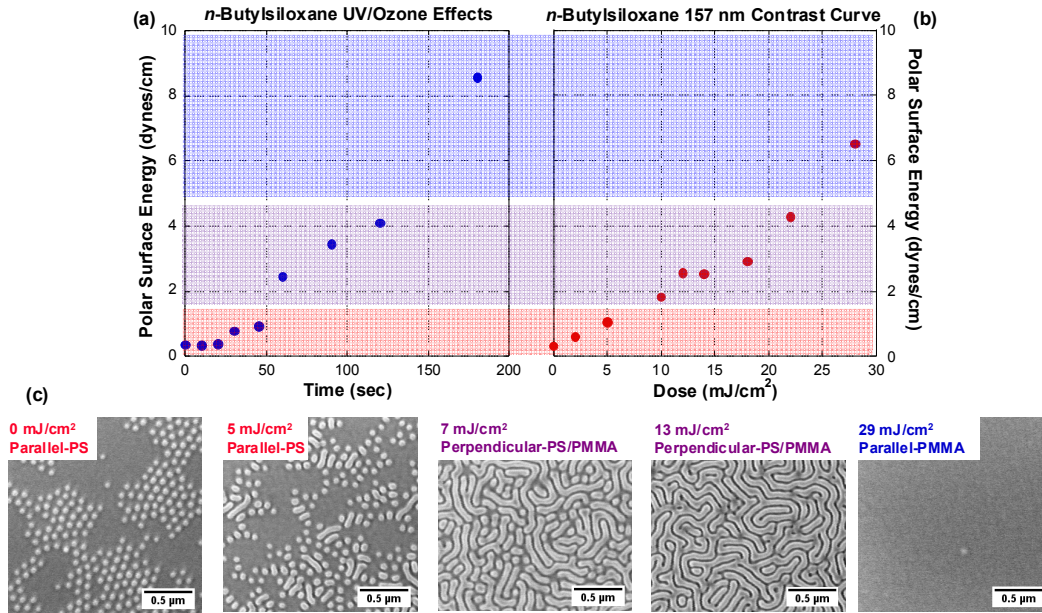


Figure 1.(a) Polar surface energy as a function of UV/ozone exposure time for an *n*-butylsiloxane-modified silicon wafer. (b) 157-nm contrast curve for an *n*-butylsiloxane-modified silicon wafer showing polar surface energy changes as a function of exposure dose. (c) SEM micrographs of 45 nm thin films of 211 kDa PS-*b*-PMMA showing changes in lamellar orientation as a function of 157-nm exposure dose.

While it is prohibitive to write an e-beam pattern with features large enough for direct surface energy measurements such as in the case of the 157-nm bulk exposure laser system, we can infer the approximate surface energies after e-beam exposure by the diblock copolymer orientation and as a function of UV/ozone development. Figure 2 shows 98.2 kDa PS-*b*-PMMA lamellar orientation after thermal annealing as a function of 157-nm exposure dose and UV/ozone treatment. At low exposure doses (<6 mJ/cm<sup>2</sup>), the PS blocks preferentially wet the substrate and small, random islands of polystyrene are observed on top of the darker PMMA lamella (not shown). Once the surface energy approaches a point that is “neutral” to both PS and PMMA (7 mJ/cm<sup>2</sup>, 1.4 dyne/cm), the lamellar orientation flips to perpendicular and the characteristic fingerprint pattern of light PS and darker PMMA domains is observed. The exposure dose window for this orientation is 7-11 mJ/cm<sup>2</sup> (1.4-2.1 dyne/cm). Defects begin to appear at 12 mJ/cm<sup>2</sup> (2.5 dyne/cm), indicating the beginning of a transition to a PMMA-preferential parallel lamellar orientation. The block copolymer film is fully parallel at higher surface energies (> 3 dyne/cm). The perpendicular lamella surface energy range for the 98 kDa PS-*b*-PMMA is lower than for the higher molecular weight 211 kDa PS-*b*-PMMA where the perpendicular lamella surface energy range was 2.9-4.9 dyne/cm (7-25 mJ/cm<sup>2</sup> exposure dose).<sup>16</sup> Thus, it seems that there is an influence of the overall block size on the surface energy compatibility of the individual styrene and methyl methacrylate blocks. Secondary exposure of surfaces that have been exposed to 157-nm irradiation results in an increase in the overall surface energy of that area. As seen in Figure 2, the dose required to change 98 kDa PS-*b*-PMMA lamellar orientation from parallel-PS preferential to perpendicular to lower exposure doses upon UV/ozone treatment. In fact, after 60 sec UV/ozone exposure, the unexposed region of an *n*-butylsiloxane surface is already in a neutral regime.

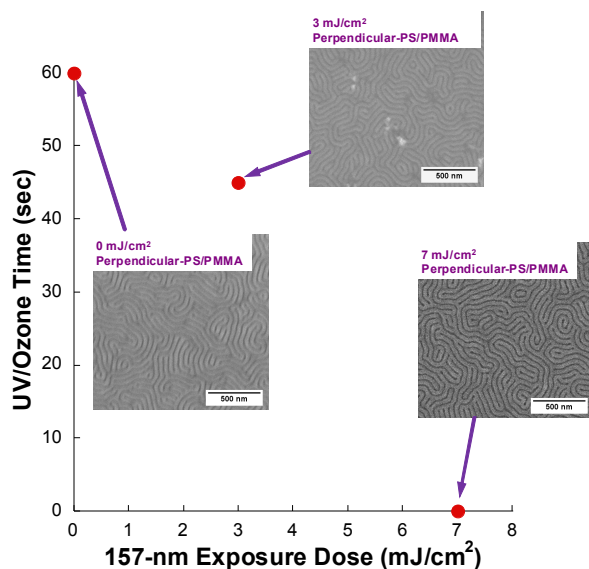


Figure 2. SEM micrographs of 45 nm thin films of 98 kDa PS-*b*-PMMA on *n*-butylsiloxane surfaces showing the initial point of perpendicular lamellar orientation as a function of 157-nm exposure dose and UV/ozone exposure time.

To investigate how e-beam exposure combined with UV/ozone changed the surface energy of the *n*-butylsiloxane surface, a series of 25  $\mu\text{m} \times 25 \mu\text{m}$  spots in increasing dose were written by e-beam lithography on these modified surfaces. The exposed areas were then UV/ozone developed for 0, 45 and 60 sec. Since we could not directly measure the polar surface energy of such a small feature size by a water drop contact angle measurement, we could infer the surface energy by block copolymer lamellar orientation. After annealing a 45 nm thick film of 98 kDa PS-*b*-PMMA, we can see the influence of electron-beam exposure and UV/ozone development on the polar surface energy (Figure 3). With no UV/ozone development, it was very difficult to locate the exposed areas on the silicon surface. We found that 45 sec UV/ozone exposure was enough to remove the carbonaceous residue left behind from e-beam exposure, but also left the surrounding *n*-butylsiloxane surface nearly unchanged. A 60 sec time was chosen to look at the influence of elevated surface energies due to the UV/ozone treatment. As can be seen in Figure 3, and similar to the case of 157-nm bulk exposure, longer UV/ozone times decreased the e-beam exposure dose required to be in the neutral surface energy regime.

We have previously shown<sup>16-17</sup> that 157-nm interference lithography can pattern an *n*-butylsiloxane surface that directs the assembly of PS-*b*-PMMA. One disadvantage of our interference lithography system is that the substrate period written by the tool is fixed, in our case at 90 nm. Still, by matching the polymer lamellar period to the substrate period, we were able to obtain defect-free aligned PS-*b*-PMMA lamella. More importantly, interference system can provide only a limited range of line-to-space ratios for any given pitch, because the aerial image is sinusoidal. Our goal, however, is to obtain asymmetric line-to-space ratios, ideally 1:3, so as to enable spatial frequency doubling of the diblock copolymer. We therefore have started exploring the use of electron-beam lithography as the templating process. It allows the flexibility to vary the substrate period to more closely match the polymer lamellar spacing as well as create uneven line and space patterns to investigate frequency multiplication. Matching the substrate period and polymer lamellar spacing is critical to reduce defects in the self-assembled PS-*b*-PMMA films.<sup>9,37-38</sup>

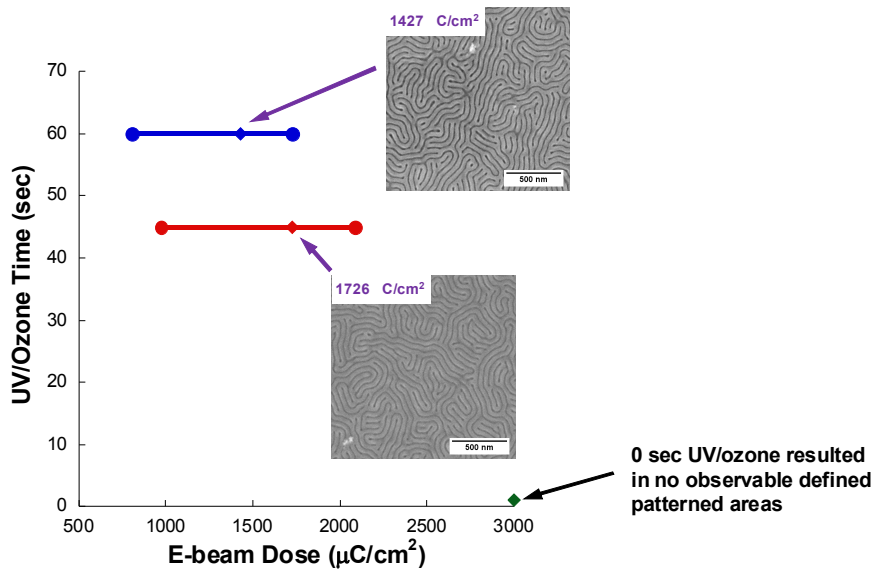


Figure 3. SEM micrographs of 45 nm thin films of 98 kDa PS-*b*-PMMA on *n*-butylsiloxane surfaces showing perpendicular lamella as a function of 50 kV electron beam dose range and UV/ozone development.

Figure 4 shows a schematic of the directed self-assembly of PS-*b*-PMMA on dense and sparse chemical patterns written by e-beam lithography. Dense chemical patterns written by e-beam lithography have the advantage of tight critical dimension control. In this case, the substrate pitch,  $P_S$ , is nearly equal to that of the lamellar spacing,  $L_O$ , of the block copolymer. The pinning line,  $W_P$ , is the feature written by the e-beam tool that is preferential to one of the blocks and directs the self-assembly of the block copolymer film, and is typically  $0.5L_O$ . There is no resolution advantage, however, of creating 1:1 patterns at these small dimensions because there is no resolution enhancement from the block copolymer, and the use of electron-beam lithography to produce these dense features is not practical for high volume production.<sup>39</sup> Sparse chemical patterns are generated where the substrate pitch is an integral multiple of the polymer lamellar period. In between the written pinning line,  $W_P$ , is a neutral surface in which the block copolymer has a preferentially perpendicular orientation.<sup>40</sup> Again, the pinning line directs the self-assembly of the block copolymer during anneal. For example, as seen in Figure 3, a pattern with  $P_S = 2L_O$  and  $W_P = 0.5L_O$  will afford frequency doubling of the written chemical pattern after block copolymer assembly.

In order to prepare surfaces that direct block copolymer self-assembly, a number of variables need to be taken into consideration, including electron-beam dose and UV/ozone development. An insufficient e-beam dose will not define the proper area to direct the self-assembly, and too much UV/ozone exposure will raise the surface energy of the unexposed areas. We therefore investigated the subtle interplay between these two treatments. Surfaces modified with *n*-butylsiloxane were exposed by electron beam lithography and developed with UV/ozone to generate thin pinning stripes with pitch ( $P_S$ ) of 45 nm and width of 22.5 nm. A number of different UV/ozone development times were investigated to determine optimal conditions that completely remove the carbon residue from e-beam exposure while not appreciably changing the remaining *n*-butylsiloxane polar surface energy. The directed assembly of a 45 nm thick film of PS-*b*-PMMA (50.6-*b*-47.6 kg/mol) was carried out at 220 °C for 2 hours. The PS-*b*-PMMA has a lamellar period ( $L_O$ ) of 45 nm, which matches the pitch of the chemical pattern. Figure 5 shows how slight changes in UV/ozone development time affect copolymer self-assembly at a given exposure dose. At lower exposure doses (2200-2400  $\mu\text{C}/\text{cm}^2$ ) fewer defects are observed at longer UV/ozone times (45 sec). This implies better removal of residual carbonaceous material left from e-beam patterning. Longer develop times at higher e-beam exposure doses seem to degrade the surface energy image, leading to numerous defects in the self-assembled film.

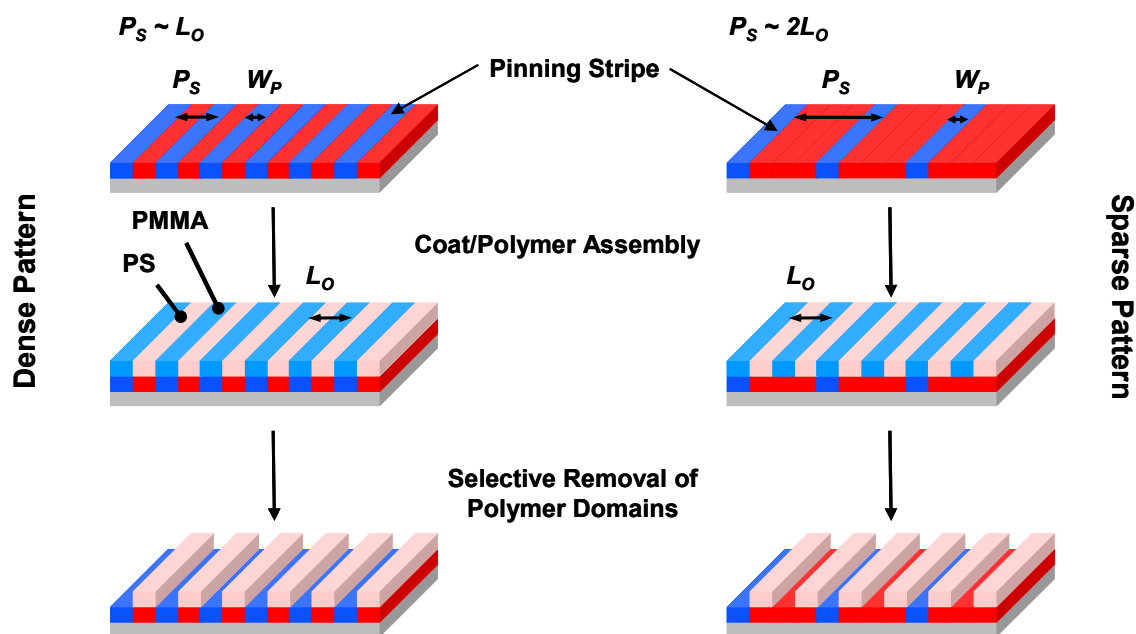


Figure 4. Schematic of directed self-assembly of PS-*b*-PMMA with lamellar spacing  $L_0$  on electron beam written chemical patterns using dense and sparse patterns.

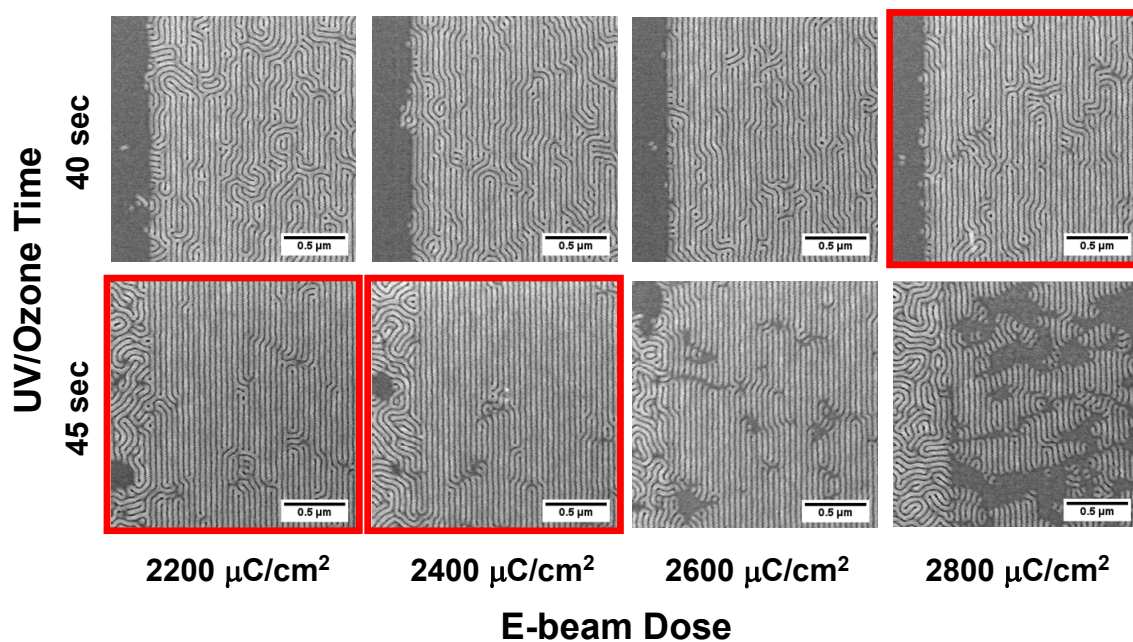


Figure 5. SEM micrographs of 45 nm thick films of PS-*b*-PMMA on *n*-butylsiloxane-modified surfaces imaged at the indicated 50 keV electron beam doses and developed with (top) 40 sec and (bottom) 45 sec UV/ozone development.

Having a chemical nanopattern pitch ( $P_S$ ) that is commensurate with the polymer lamellar period ( $L_O$ ) is critical for forming defect-free self-assembled films.<sup>9,37-38</sup> Randomly assembled films of 98 kDa PS-*b*-PMMA (50.6-*b*-47.6) have shown a lamellar period of 45 nm as measured by SEM. When chemically nanopatterned surfaces having a pinning line width ( $W_P$ ) of 22.5 nm and pitch ( $P_S$ ) of 45 nm are used, numerous dislocation defects are observed, even in the best films processed (Figure 5). Since these block copolymer films have the ability to expand or contract lamellar spacing depending on the surface conditions, we investigated the effect of slightly changing the substrate pitch while keeping the pinning line width constant. Films of 45-nm thick PS-*b*-PMMA were annealed on electron-beam generated chemical nanopatterns with a  $W_P$  of 22.5 nm and  $P_S$  of 42.5, 45.0, and 47.5 nm. As seen in Figure 6, for a given electron-beam exposure dose, films with  $P_S$  of 47.5 nm had consistently fewer defects than for  $P_S$  of 45.0 nm. Having an even smaller substrate pitch (42.5 nm) resulted in an even larger number of defects.

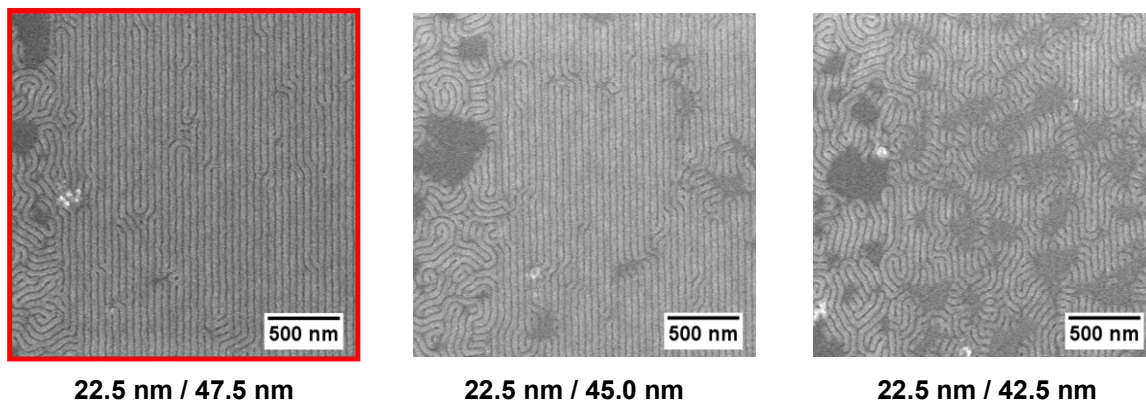


Figure 6. SEM micrographs of 45 nm thick films of PS-*b*-PMMA on *n*-butylsiloxane-modified surfaces imaged at 2480  $\mu\text{C}/\text{cm}^2$  at 50 keV showing the effect of chemical nanopattern pitch with a constant 22.5 nm pinning line with a variable pitch ranging from 42.5 nm to 47.5 nm on polymer self-assembly.

Copolymer film thickness plays a crucial role in how well the surface chemical nanopattern translates to the polymer-air interface. If the film is too thick, incomplete assembly at the surface is observed, even though the polymer near the substrate is aligned with the chemical nanopattern.<sup>41-43</sup> Thinner films should have uniform lamellar domains that extend from the substrate to the air interface. Films of PS-*b*-PMMA were spun to thicknesses of 30, 45, and 63 nm on chemically nanopatterned substrates and annealed to investigate the effect of film thickness. Figure 7 shows how the film thickness directly relates to the amount of defects in the resulting self-assembled films. Thinner films (30 nm) showed nearly defect-free self-assembled lamella, while moderate and thick films (45 and 63 nm) showed increasing number of defects with increasing film thickness.

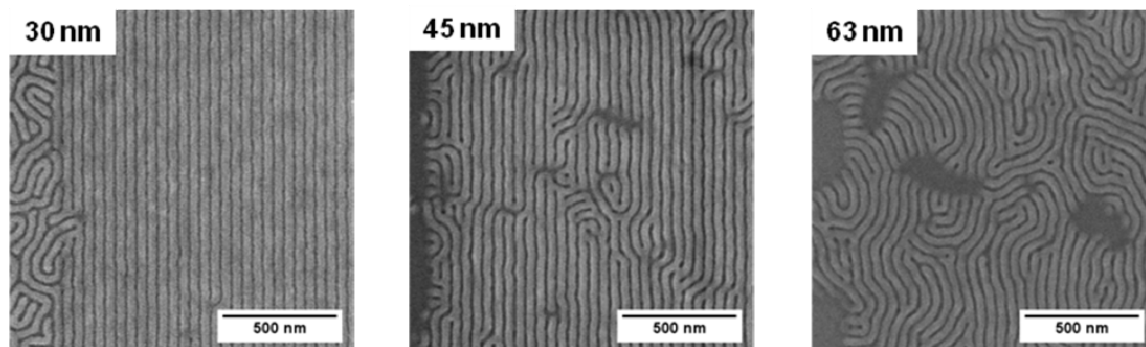


Figure 7. SEM micrographs of PS-*b*-PMMA films on *n*-butylsiloxane-modified surfaces imaged at 4500  $\mu\text{C}/\text{cm}^2$  at 50 keV showing the effect of block copolymer film thickness on polymer self-assembly.

The ultimate goal of using electron beam lithography to generate chemical nanopatterns is to form sparse chemical patterns that direct frequency multiplication with smaller block copolymer films. This approach has been investigated at IBM by Cheng *et al.*,<sup>39</sup> where they patterned a thin HSQ pinning line over a neutral random copolymer brush that is grafted to the substrate. Through judicious choice of the chemical nanopattern pitches ( $P_S$ ) that are integral multiples of the block copolymer lamellar period ( $L_O$ ), the IBM group was able to show defect free frequency multiplication in both straight line patterns as well as curved patterns.<sup>39</sup> Our approach, similar to our approach with optical lithographically directed assembly, was to forgo the additional steps of attaching a random copolymer and then pattern the HSQ pinning line before block copolymer self-assembly. We envisioned that directly patterning the *n*-butylsiloxane-modified surface with an asymmetric chemical nanopattern would also result in frequency multiplication if the substrate pitch was chosen correctly. Our initial experiments have met with mixed success. Chemical nanopatterns having  $P_S$  of 95 nm were generated by e-beam patterning of an *n*-butylsiloxane-modified substrate, followed by UV/ozone development. Films of 98 kDa PS-*b*-PMMA that were 30 nm thick were spin cast and then annealed at 260 °C for 2 hrs under nitrogen. The resulting patterns are shown in Figure 8. As can be observed, there is an overall direction to the annealed lamellar domains, but with numerous dislocation defects. These are our first results, and we expect that the defects are due to a number of unoptimized process factors, with the most obvious being a mismatch between polymer lamella spacing ( $L_O$ ) and the written pitch ( $P_S$ ). These results, however, do show promise that our method of direct chemical patterning can result in frequency multiplication with PS-*b*-PMMA films. Future work will focus on fine tuning this process to generate defect-free films.

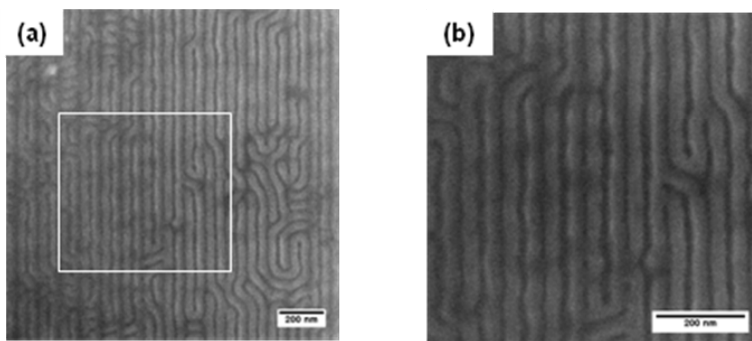


Figure 8. (a) SEM micrographs of 30 nm thick films of PS-*b*-PMMA on *n*-butylsiloxane-modified surfaces imaged at with a pinning line width ( $W_P$ ) of 22.5 nm and a pitch ( $P_S$ ) of 95 nm. (b) Higher magnification SEM micrograph of the outlined region in (a).

#### 4. SUMMARY

Silicon wafers coated with surface modifying agents can be directly imaged by electron-beam lithography to produce surfaces to direct the self-assembly of PS-*b*-PMMA films in similar fashion to our prior work with 157-nm optical lithography. UV/ozone development of electron-beam patterned areas was shown to be an important step in generating well-defined areas of proper surface energy to direct the self-assembly of PS-*b*-PMMA films into ordered lamellae. Both block copolymer film thickness and the chemical nanopattern pitch were shown to be important factors in generating defect-free films. Our initial experiments with frequency multiplication using this technique led to films with numerous dislocation defects, but general lamellar ordering has been obtained. They indicate that, with appropriate material and process optimization, direct surface imaging of a siloxane-modified substrate is a viable route to frequency multiplication and generating smaller feature sizes.

#### 5. ACKNOWLEDGMENTS

We would like to thank Al Cabral for help with surface energy measurements and Susan Cann for SEM assistance. This work was sponsored by the Defense Advanced Research Projects Agency under Air Force Contract FA8721-05-C-0002. Opinions, interpretations, conclusions, and recommendations are those of the author, and do not necessarily represent the view of the United States Government.

## REFERENCES

- [1] Bates, F. S. and Fredrickson, G. H., "Block Copolymer Thermodynamics: Theory and Experiment," *Annu. Rev. Phys. Chem.* 41, 525-557 (1990).
- [2] Park, M., Harrison, C., Chaikin, P. M., Register, R. A., and Adamson, D. H. "Block Copolymer Lithography: Periodic Arrays of ~ 1011 Holes in 1 Square Centimeter," *Science* 276(5317), 1401-1404 (1997).
- [3] Kim, S. O., Solak, H. H., Stoykovich, M. P., Ferrier, N. J., de Pablo, J. J. and Nealey, P. F., "Epitaxial self-assembly of block copolymers on lithographically defined nanopatterned substrates," *Nature* 424(6947), 411-414 (2003).
- [4] Edwards, E. W., Montague, M. F., Solak, H. H., Hawker, C. J. and Nealey, P. F., "Precise control over molecular dimensions of block-copolymer domains using the interfacial energy of chemically nanopatterned substrates," *Adv. Mater.* 16(15), 1315-1319 (2004).
- [5] Edwards, E. W., Müller, M., Stoykovich, M. P., Solak, H. H., de Pablo, J. J. and Nealey, P. F., "Dimensions and shapes of block copolymer domains assembled on lithographically defined chemically patterned substrates," *Macromolecules* 40(1), 90-96, (2007).
- [6] Ruiz, R., Ruiz, N., Zhang, Y., Sandstrom, R. L. and Black, C. T., "Local defectivity control of 2D self-assembled block copolymer patterns," *Adv. Mater.* 19(16), 2157-2162 (2007).
- [7] Stoykovich, M. P., Kang, H., Daoulas, K. C., Liu, G., Liu, C. -C., de Pablo, J. J., Müller, M. and Nealey, P. F., "Directed self-assembly of block copolymers for nanolithography: fabrication of isolated features and essential integrated circuit geometries," *ACS Nano* 1(3), 168-175 (2007).
- [8] Welander, A. M., Kang, H., Stuen, K. O., Solak, H. H., Müller, M., de Pablo, J. J. and Nealey, P. F., "Rapid directed assembly of block copolymer films at elevated temperatures," *Macromolecules* 41(8), 2759-2761 (2008).
- [9] Edwards, E. W., Stoykovich, M. P., Nealey, P. F. and Solak, H. H., "Binary blends of diblock copolymers as an effective route to multiple length scales in perfect directed self-assembly of diblock copolymer thin films," *J. Vac. Sci. Technol. B* 24(1), 340-344 (2006).
- [10] Hawker, C. J., Russell, T. P., "Block Copolymer Lithography: Merging Bottom-Up with Top-Down Processes," *MRS Bulletin* 30(12), 952-966 (2005).
- [11] Black, C. T., Ruiz, R., Breyta, G., Cheng, J. Y., Colburn, M. E., Guarini, K. W., Kim, H. -C. and Zhang, Y. "Polymer self assembly in semiconductor microelectronics," *IBM J. Res & Dev.* 51(5), 605-633 (2007).
- [12] Yang, X. M., Peters, R. D., Nealey, P. F., Solak, H. H. and Cerrina, F., "Guided self-assembly of symmetric diblock copolymer films on chemically nanopatterned substrates," *Macromolecules* 33(26), 9575-9582 (2000).
- [13] Kim, S.-J., Maeng, W. J., Lee, S. K., Park, D. H., Bang, S. H., Kim, H. and Sohn, B.-H. "Hybrid nanofabrication processes utilizing diblock copolymer nanotemplate prepared by self-assembled monolayer based surface neutralization," *J. Vac. Sci. Technol. B* 29(1), 189-194 (2008).
- [14] Sohn, B. H. and Yun, S. H. "Perpendicular lamellae induced at the interface of neutral self-assembled monolayers in thin diblock copolymer films," *Polymer* 43, 2507-2512 (2002).
- [15] Park, D.-H. "The fabrication of thin films with nanopores and nanogrooves from block copolymer thin films on the neutral surface of self-assembled monolayers," *Nanotechnology* 19, 355304 (2007).
- [16] Kingsborough, R. P., Goodman, R. B., Krohn, K. and Fedynyshyn, T. H. "Lithographically directed materials assembly," *Proc. SPIE* 7271, 72712D (2009).
- [17] Kingsborough, R. P., Goodman, R. B. and Fedynyshyn, T. H. "Lithographically directed surface modification," *J. Vac. Sci. Technol. B* 27(6), 3031-3037 (2009).
- [18] Smith, R. K., Lewis, P. A. and Weiss, P. S. "Patterning self-assembled monolayers," *Prog. Surf. Sci.* 75(1-2), 1-68 (2004).
- [19] Sugimura, H., Ushiyama, K., Hozumi, A. and Takai, O. "Micropatterning of alkyl- and fluoroalkylsilane self-assembled monolayers using vacuum ultraviolet light," *Langmuir* 16(3), 885-888 (2000).
- [20] Nae, F. A., Saito, N., Hozumi, A. and Takai, O. "High resolution submicron patterning of self-assembled monolayers using a molecular fluorine laser at 157 nm," *Langmuir* 21(4), 1398-1402 (2005).
- [21] Nae, F. A., Saito, N. and Takai, O. "Submicron optical near-field diffraction patterns obtained by irradiation of octadecyltrimethoxysilane self-assembled monolayers with light at 157 nm," *Thin Solid Films* 515(12), 5147-5152 (2007).

- [22] Chen, M.-S., Dulcey, C. S., Chrisey, L. A. and Dressick, W. J., "Deep-UV photochemistry and patterning of (aminoethylaminomethyl)phenethylsiloxane self-assembled monolayers," *Adv. Funct. Mater.* 16(6), 774-783 (2006).
- [23] Dulcey, C. S., Georger Jr., J. H., Krauthamer, V., Stenger, D. A., Fare, T. L. and Calvert, J. M. "Deep UV photochemistry of chemisorbed monolayers: patterned coplanar molecular assemblies," *Science* 252(5005), 551-554 (1991).
- [24] Dulcey, C. S., Georger Jr., J. H., Chen, M. -S., McElvany, S. W., O'Ferrall, C. E., Benezra, V. I. and Calvert, J. M. "Photochemistry and patterning of self-assembled monolayer films containing aromatic hydrocarbon functional groups," *Langmuir* 12(6), 1638-1650 (1996).
- [25] Ingall, M. D. K., Honeyman, C. H., Mercure, J. V., Bianconi P. A. and Kunz, R. R. "Surface functionalization and imaging using monolayers and surface-grafted polymer layers," *J. Am. Chem. Soc.* 121(15), 3607-3613 (1999).
- [26] Dressick, W. J., Dulcey, C. S., Chen, M. -S. and Calvert, J. M. "Photochemical studies of (aminoethylaminomethyl) phenethyltrimethoxysilane self-assembled monolayer films," *Thin Solid Films* 284-285, 568-572 (1996).
- [27] Friebel, S., Aizenberg, J., Abad, S. and Wiltzius, P. "Ultraviolet lithography of self-assembled monolayers for submicron patterned deposition," *Appl. Phys. Lett.* 77(15), 2406-2408 (2000).
- [28] Friedli, A. C., Roberts, R. D., Dulcey, C. S., Hsu, A. R., McElvany, S. W. and Calvert, J. M. "Photochemistry and patterning of monolayer films from 11-phenylundecyltrichlorosilane," *Langmuir* 20(10), 4295-4298 (2004).
- [29] Harnett, C. K., Satyalakshmi, K. M. and Craighead, H. G., "Bioactive templates fabricated by low-energy electron beam lithograph of self-assembled monolayers," *Langmuir* 17(1), 178-182 (2001).
- [30] Zhang, G.-J., Tanii, T., Zako, T., Hosaka, T., Miyake, T., Kazari, Y., Funatsu, T. and Ohdomari, I., "Nanoscale patterning of protein using electron beam lithography of organosilane self-assembled monolayers," *Small* 1(8-9), 833-837 (2005).
- [31] Lercel, M. J., Whelan, C. S., Craighead, H. C., Seshadri, K. and Allara, D. L. "High-resolution silicon patterning with self-assembled monolayer resists," *J. Vac. Sci. Technol. B* 14(6), 4085-4090 (1996).
- [32] Whelan, C. S., Lercel, M. J., Craighead, H. G., Seshadri, K. and Allara, D. L. "Improved electron-beam patterning of Si with self-assembled monolayers," *Appl. Phys. Lett.* 69(27), 4245-4247 (1996).
- [33] Seshadri, K., Froyd, K., Parikh, A. N., Allara, D. L., Lercel, M. J. and Craighead, H. G. "Electron-beam induced damage in self-assembled monolayers" *J. Phys. Chem.* 100(39), 15900-15909 (1996).
- [34] Bikerman, J. J., "Measuring contact angles," *Ind. Eng. Chem., Anal. Ed.* 13, 443-444 (1941).
- [35] Fowkes, F. M., "Determination of interfacial tensions, contact angles, and dispersion forces in surfaces by assuming additivity of intermolecular interactions in surfaces," *J. Phys. Chem.* 66, 382 (1962).
- [36] Fowkes, F. M., "Additivity of intermolecular forces at interfaces. I. Determination of the contribution to surface and interfacial tensions of dispersion forces in various liquids," *J. Phys. Chem.* 67(12), 2538-2541 (1963).
- [37] Kim, S. O., Kim, B. H., Kim, K., Koo, C. M., Stoykovich, M. P., Nealey, P. F. and Solak, H. H., "Defect structure in thin films of a lamellar block copolymer self-assembled on neutral homogeneous and chemically nanopatterned substrates," *Macromolecules* 39(16), 5466-5470 (2006).
- [38] Stoykovich, M. P., Müller, M., Kim, S. O., Solak, H. H., Edwards, E. W., de Pablo, J. J. and Nealey, P. F., "Directed assembly of block copolymer blends into nonregular device oriented structures," *Science* 308(5727), 1442-1446 (2005).
- [39] Cheng, J. Y., Rettner, C. T., Sanders, D. P., Kim, H.-C. and Hinsberg, W. D. "Dense self-assembly on sparse chemical patterns: rectifying and multiplying lithographic patterns using block copolymers," *Adv. Mater.* 20(16), 3155-3158 (2008).
- [40] Mansky, P., Liu, Y., Huang, E., Russell, T. P. and Hawker, C. "Controlling polymer-surface interactions with random copolymer brushes," *Science* 275(5305), 1458-1460 (1997).
- [41] Huang, E., Mansky, P., Russell, T. P., Harrison, C., Chaikin, P. M., Register, R. A., Hawker, C. J. and Mays, J. "Mixed lamellar films: evolution, commensurability effects, and preferential defect formation," *Macromolecules*, 33(1), 80-88 (2000).
- [42] Rockford, L., Mochrie, S. G. J. and Russell, T. P. "Propagation of nanopatterned substrate template ordering of block copolymers in thick films," *Macromolecules* 34(5), 1487-1492 (2001).
- [43] Xu, T., Hawker, C. J. and Russell, T. P. "Interfacial interaction dependence of microdomain orientation in diblock copolymer thin films," *Macromolecules* 38(7), 2802-2805 (2005).